JOURNAL OF CATALYSIS 135, 345–357 (1992)

Catalytic Oxidation of Organics in Aqueous Solutions

I. Kinetics of Phenol Oxidation

A. PINTAR AND J. LEVEC*

*Laboratory of Catalysis and Chemical Reaction Engineering, Boris Kidrič Institute of Chemistry, Ljubljana, Slovenia; and *Department of Chemical Engineering, University of Ljubljana, P.O. Box 537, 61001 Ljubljana, Slovenia*

Received March 26, 1991; revised January 22, 1992

Liquid-phase oxidation using a solid catalyst provides a potential method for removal of dissolved toxic organic pollutants from waste waters. Catalytic oxidation of phenol in an aqueous solution was studied in a semibatch slurry reactor. A catalyst comprising ZnO, CuO, and Al_2O_3 was found to be effective for converting phenol to nontoxic compounds via different intermediate products at pressures slightly above atmospheric and temperatures below 130°C. Rate measurements showed that the reaction progressed autocatalytically and involved a heterogeneous–homogeneous free radical mechanism and stepwise addition polymerization. The proposed rate equation for the phenol disappearance, which exhibits linear behavior with respect to the phenol concentration and one-fourth power of the oxygen partial pressure, is expressed in terms of the initial phenol concentration as well as the catalyst concentration. Apparent activation energy for the catalytic oxidation of phenol was found to be 84 kJ/mol in a temperature range of 105 to 130°C.

INTRODUCTION

In petrochemical, chemical, and pharmaceutical industries there are waste waters containing organics in concentrations far too low for them to be economically recoverable, yet in concentrations so high that they pollute the environment. Since industrialized countries now wish to achieve a "zero pollutant" discharge, the inability to effectively remove many refractory organics by conventional methods has made it evident that new and more efficient systems are needed.

Apart from biological and chemical oxidation processes, several systems are used or are in various stages of development. For example, thermal liquid-phase or wet air oxidation processes are known to have great potential in advanced waste treatment facilities. Reaction conditions as severe as 200–300°C and 70–130 bar and the presence of a wide range of oxygenated compounds, which are highly corrosive, considerably affect the economics of the process. Photoassisted heterogeneous catalytic destruction of halogenated and aromatic hydrocarbons also has been gaining attention as a technique for purifying waste waters (*1*).

An alternative process to the thermal liquid-phase oxidation of refractory organics in waste waters is catalytic oxidation (*2–4*). In this process refractory organics are oxidized to carbon dioxide and water over a solid catalyst in a three-phase system with milder conditions than those found in the thermal process. The key issue in the catalytic oxidation process is a catalyst. The conditions under which small amounts of organics dissolved in a large amount of water are oxidized force a severe demand on the physical and chemical properties of a catalyst. Hot acidic aqueous solutions can promote the solubility of some metal oxides in their higher oxidation states and consequently, deactivate an otherwise favorable catalyst. Metals present in waste water may also deactivate a catalyst.

0021-9517/92 $5.00

In comparison with the numerous studies for pure organic liquids, relatively few investigations have been published for oxidation of organic compounds in aqueous solutions. Very few quantitive rate data are found. Rate equations for the liquid-phase catalytic oxidation have been published for model pollutants such as formic acid, acetic acid, and phenol. The kinetic results of these investigations can be summarized as follows:

- Formic acid oxidation (*5*) is first order with respect to both oxygen partial pressure and formic acid concentration (catalyst: $CuO \cdot ZnO$).
- Acetic acid oxidation (*6, 7*) can be well described by the Langmuir–Hinshelwood mechanism (catalysts: Fe_2O_3 and $ZnAl_2O_4$ promoted by Mn and La).
- The phenol catalytic oxidation undergoes an induction period with transition to a much higher steady-state activity regime. This reaction is first order with respect to phenol in both regimes, but the oxygen dependence decreases from first to one-half order in shifting from the induction period to the steady-state activity regime (*8, 9*). However, Ohta *et al.* (*10*) have found different kinetic behavior with the same catalyst (CuO on γ-Al_2O_3).

In order to develop an effective catalytic process for purifying industrial waste waters, more kinetic and mechanistic studies with different systems in aqueous solution are needed. The purpose of this work is to present thorough kinetic studies of the catalytic oxidation of some refractory organics found frequently in industrial waste waters (e.g., phenols, nitrophenols, chlorophenols, tertiary butyl alcohol, methyl vinyl ketone, naphthalene sulfonate) aimed at the development of rate equations for the oxidation reactor design. Initially, the kinetics and reaction pathway of phenol oxidation using $CuO \cdot ZnO \cdot Al_2O_3$ are discussed. The kinetics of catalytic oxidation for other listed pollutants will be introduced in subsequent papers.

EXPERIMENTAL

Catalyst

The liquid-phase oxidation of phenol by oxygen was studied using a commercially available, low-temperature CO conversion catalyst (G-66A, Süd-Chemie AG, Munich, Germany) comprising 42 wt% of CuO, 47 wt% of ZnO, and 10 wt% of Al_2O_3. In preliminary experiments, it was found that the catalyst is the most active when it is pretreated for 2 h at 860°C in an oxygen stream and then cooled to room temperature (*11, 12*).

XRD examination of the calcined catalyst samples showed that during the process two spinels were formed, $ZnAl_2O_4$ and $CuAl_2O_4$. The latter is present in only small amounts. Formation of a new phase also was confirmed by SEM micrographs. The catalyst pretreated at 860°C contains approximately 16 wt% of $ZnAl_2O_4$, 60 wt% of CuO, and 24 wt% of ZnO. The surface area (BET) of the pretreated catalyst was 11.1 m^2/g.

Apparatus

Kinetic experiments were carried out in a 2-liter stainless-steel reactor equipped with a magnetically driven turbine type impeller and temperature and pressure control units (Parr Instrument Company, IL). The temperature of the reaction mixture was maintained within ∓ 1 K of the set value. The total pressure in the system was kept constant by a back-pressure regulator (Tescom Corporation, MN), the deviation not exceeding $\mp 0.5\%$ of the set pressure. The oxygen flow, introduced into the vessel below the impeller, was controlled by an electronic mass flow controller (Brooks). Since three phases were present in the reactor, the entire system is treated as a slurry reactor. The apparatus is schematically shown in Fig. 1.

Experimental Procedure

In a typical run a given amount of fresh catalyst was charged into the reactor containing 1.3 liter of distilled water with a given amount of phenol. The range of experimen-

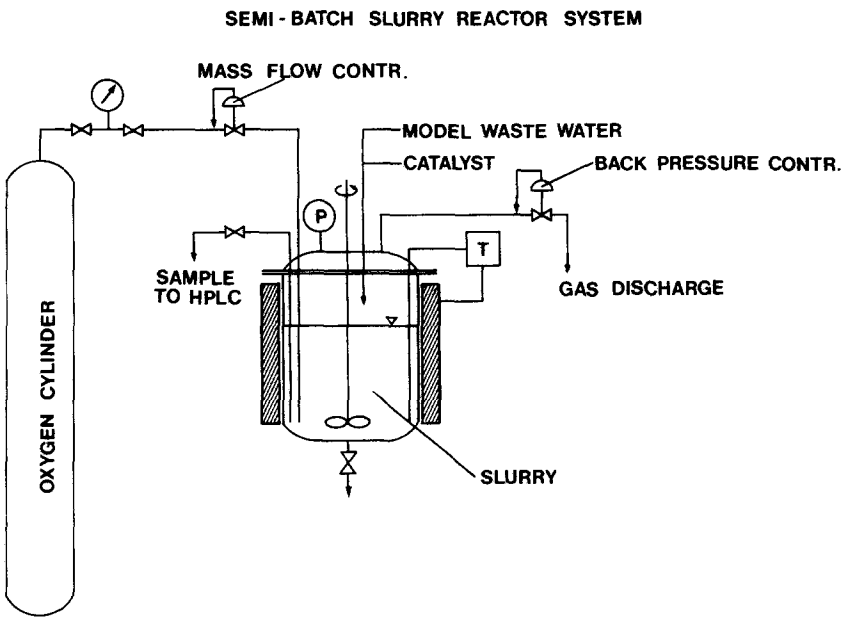

FIG. 1. Apparatus for phenol catalytic oxidation studies using semibatch slurry reactor system.

tal conditions used in this work is shown in Table 1. The back-pressure regulator was set and the content of the reactor was brought to reaction conditions. Then oxygen was sparged continuously through the suspension at a metered rate. Representative samples were withdrawn periodically (the time period was a function of experimental conditions) and the catalyst was immediately separated from the aqueous phase by centrifugation. The aqueous phase was diluted and then analyzed for residual content of phenol, intermediate products, and total organic carbon.

TABLE 1

Range of Operating Conditions

Initial phenol concentration	0.02–0.101 mol/liter
Catalyst concentration	3.0–11.0 g/liter
Particle diameter	<0.075 mm
Oxygen flow rate (STP conds.)	1.0 and 3.0 liter/min
Oxygen partial pressure	1.5–10.0 bar
Total pressure	4.6–13.1 bar
Temperature	105–130°C
pH	5.5 and 7.3
Stirrer speed	600–1300 rpm

External mass transfer resistance can be dependent on stirrer speed. Runs were made for various stirrer speeds and for different oxygen flow rates with resulting rates of phenol oxidation independent of both these variables in the range investigated (Table 1). The amount of phenol disappeared in a blank run was certainly within experimental errors.

Analysis

Residual phenol concentrations in diluted samples were determined by HPLC using LiChrosorb RP-18 (Merck) as a stationary phase, while the mobile phase was a mixture of LiChrosolv (Merck) and bidistilled water (in ratio 1 : 1). Flow rate of the mobile phase was equal to 60 ml/h. An UV spectrophotometer at $\lambda = 270$ nm was employed as a detector.

The amount of CO_2 generated during an experiment was determined gravimetrically. The reactor gas outlet stream was continuously bubbled into a saturated barium

hydroxide solution. The precipitate was then filtered, washed, dried, and weighed. The amount of organic compounds adsorbed on the catalyst was determined by Perkin–Elmer 2400 CHN elemental analyzer. The aqueous phase samples were evaluated for total organic carbon concentrations. Analyses were performed on a Beckman total organic carbon analyzer.

Identification of intermediate products, formed during the course of phenol oxidation, were performed on Hewlett–Packard GC(5980A)/MSD(5970) system. A HP-5 (Ultra-2) column (25m · 0.32 mm · 0.52 μm) was used with a helium flow of 1 ml/min. The temperatures of the injector and the interface were 230 and 260°C, respectively. Oven temperature was 70°C for the first 2 min, increasing at a rate of 20°C/min until 280°C was reached. The sample volume was 1 μl. Intermediates were identified by comparing a spectrum for a particular compound with spectra of compounds stored in the NBS library.

RESULTS AND DISCUSSION

Reaction Pathway

By means of GC/MSD analysis the following intermediates were detected during the course of phenol oxidation: 2,5-cyclohexadiene-1,4-dione, 1,2-benzenediole, 1,4-benzenediole, acetic acid, and carbon dioxide. The intermediate 2,5-cyclohexadiene-1,4-dione was found in very low concentrations, but acetic acid was usually present in relatively high concentrations. This was not surprising since it is quite refractory for the oxidation (*6*). Sadana and Katzer (*8, 9*) also found 2,5-cyclohexadiene-1,4-dione and 3,5-cyclohexadiene-1,2-dione, while Ohta *et al.* (*10*) detected both benzenedioles. In the present work no maleic acid was detected. It appears that maleic acid is formed only when phenol is oxidized by V_2O_5 catalyst (*13*).

Oxidation of phenol exhibits an induction period (Figs. 4 and 5) with the rate dependent on the catalyst concentration (Fig. 10) and the initial phenol concentration (Fig. 11). Furthermore, the reaction rate was accelerated appreciably (no induction period) when a small amount of H_2O_2 (0.1 wt%) was added to the phenol solution prior to starting a kinetic run. It is therefore speculated that the catalytic phenol oxidation undergoes a heterogeneous–homogeneous free radical mechanism. This also has been suggested by other investigators (*8, 9*). Radicals can be generated on solid catalyst surface by two methods (*3, 9*): (1) the catalyst activates reactant molecules directly, and facilitates their decomposition into radicals, or (2) the catalyst accelerates the decomposition of hydroperoxides into radicals, the hydroperoxides being either present in the system or formed slowly by the first mechanism. If the first method is assumed, radicals on the catalyst surface can be formed by the reaction

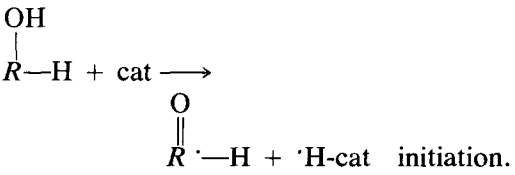

initiation.

Thus, formed radicals may further react with oxygen in the liquid phase and produce peroxy radicals

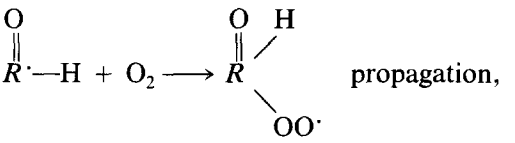

propagation,

where –OO· is located in the *ortho-* or *para-*position. Peroxy radicals react in the liquid phase with phenol molecules

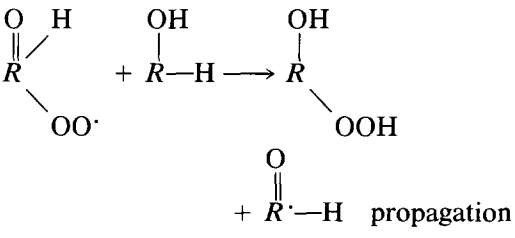

propagation

and form hydroperoxide. It is further oxidized to benzenedioles and other products. In the above reactions RH–OH refers to

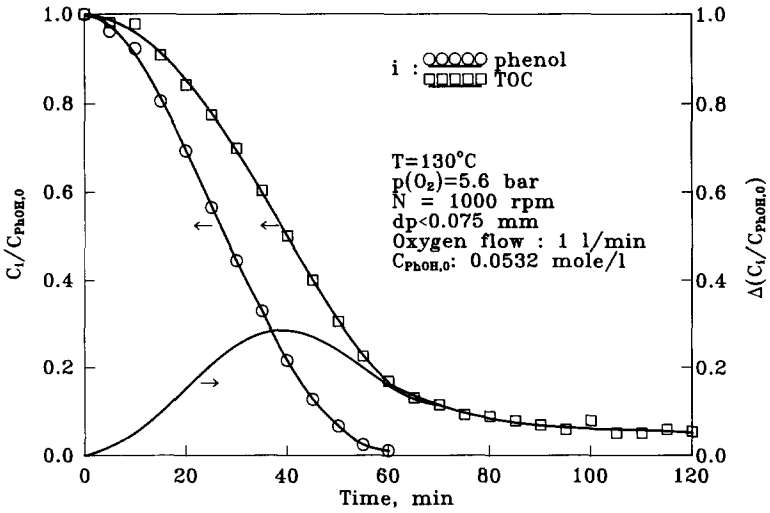

FIG. 2. Relative TOC and phenol concentrations vs time. Cat. conc., 5 g/liter.

phenol, RH=O· to the phenoxy radical, and RHO–OO· to the peroxy radical. It should be noted that the involvement of surface-adsorbed oxygen represents another possible propagation pathway (*9*). However, it is beyond the scope of this paper to speculate on the reaction mechanism in detail; it is discussed elsewhere (*8, 9, 14*).

The difference between TOC and phenol concentrations (Fig. 2) indicates that some intermediate products were accumulated in the liquid phase during the oxidation. On the other hand, only 22% of phenol was converted to CO_2 in the first hour, and 40% after 5 h of reaction time had elapsed. The rest of the organic carbon was found in a polymeric product strongly adsorbed on the catalyst and not soluble in conventional organic solvents. The NMR ^{13}C CPMAS examination of the adsorbed product indicated that it was formed by two reactions carried out in the liquid phase: (1) stepwise addition polymerization of the C-2 aldehyde (glyoxale) to phenol and (2) polymerization of the C-2 aldehyde. It was estimated quantitatively from the NMR spectra that the polymer was mainly derived from the first reaction. However, in a typical run after 1 h of the reaction time 47 wt% of initial carbon was found on the catalyst surface (CHN analyzer), 18 wt% in the aqueous phase (TOC), and 22 wt% in the gaseous phase as CO_2. The rest of the carbon was adsorbed as a polymeric product on the reactor wall and could not be evaluated quantitatively.

Based on the intermediates and products detected, the catalytic oxidation of phenol may obey a parallel–consecutive reaction scheme as shown in Fig. 3. Phenol disappears by the two reaction routes: (1) it is catalytically oxidized via intermediates to glyoxale and (2) it is consumed by the stepwise addition polymerization in the liquid phase. A polymer is initiated by the reaction between glyoxale and phenol. It is believed that glyoxale is further oxidized to carbon dioxide also by a heterogeneous reaction. According to the experimental observations discussed in the next section the autocatalytic behavior of the system can be, however, attributed to a stepwise addition polymerization. It should be noted that a polymeric product was also found on the catalyst surface when aqueous solutions of pure 2,5-cyclohexadiene-1,4-dione and pure glyoxale were oxidized. The polymerization may be promoted by acidic sites on the catalyst surface; a blockade of these sites by

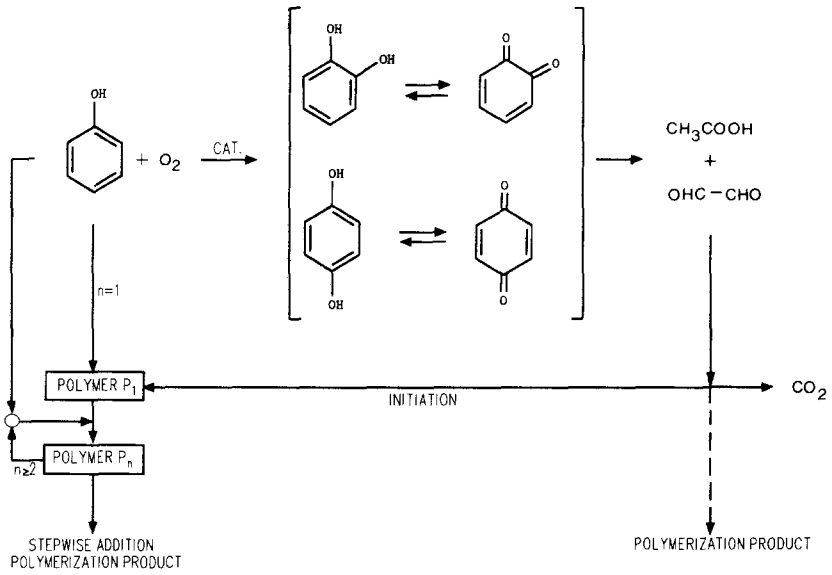

FIG. 3. Proposed reaction pathway of phenol oxidation over $CuO \cdot ZnO \cdot Al_2O_3$ catalyst.

sodium carbonate (pH 7.3) did not prevent formation of the polymeric product. The induction period was considerably extended in this particular experiment, agreeing with the results of Sadana and Katzer (*9*). The polymeric product had deactivated the catalyst after the second consecutive run with the same catalyst batch. Nevertheless, the catalyst can be regenerated easily by burning out the polymeric product.

Reaction Kinetics

Figure 4 shows the phenol concentration as a function of time at different reaction temperatures with a constant oxygen pressure. Figure 5 represents the same dependence at different oxygen partial pressures but a constant reaction temperature (experimental points). Data on Figs. 4 and 5 illustrate typical concentration–time behavior for an autocatalytic reaction. This can be confirmed by differentiating the concentration vs time curves and plotting the obtained derivatives against the phenol concentration. The resulting parabolic rate–concentration curves, characteristic of autocatalysis, are depicted in Fig. 6. Each curve arrives at maximum practically at $c_{PhOH}/c_{PhOH,0} = 0.50$.

According to the proposed reaction scheme the rate of phenol disappearance may be written as

$$(-r_{PhOH}) = -\frac{1}{c_{cat.}} \cdot \frac{dc_{PhOH}}{dt} = k' \cdot f(p(O_2)) \cdot c_{PhOH} + k \cdot c_{PhOH} \cdot \sum_n c(P_n), \quad (1)$$

where k' is the rate constant for the heterogeneous oxidation and k is the lump polymerization rate constant including initiation (phenol plus glyoxale) and propagation steps. The total molar concentration of reactive polymer containing n molecules of phenol, which appears in Eq. (1), can be evaluated from a mass balance on phenol. Since phenol must be in either the monomer or the polymer form as well as in intermediate and other product forms, it follows that

$$M_{PhOH} \cdot (c_{PhOH,0} - c_{PhOH}) = \sum_n M_n \cdot c(P_n) + \sum_i \frac{M_i}{\nu_i} \cdot c_i, \quad (2)$$

where the contribution of oxygen to the mo-

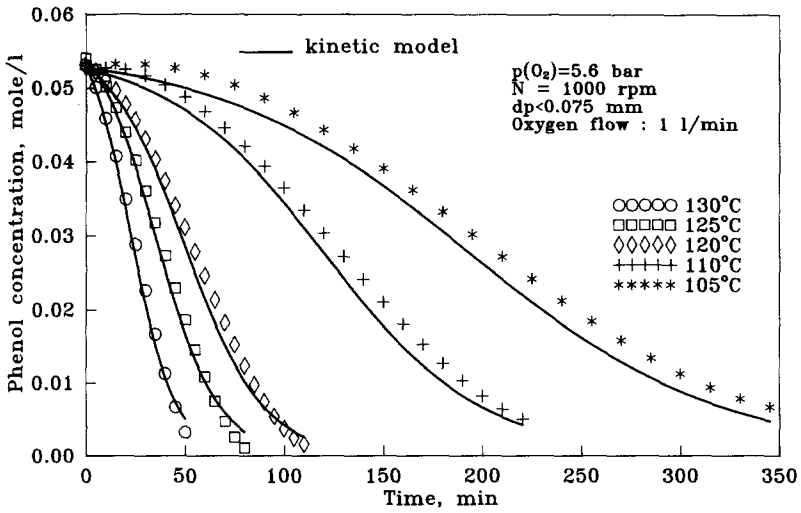

FIG. 4. Residual phenol concentration as a function of time at different reaction temperatures and $p(O_2)$ = 5.6 bar. Cat. conc., 5 g/liter. Initial phenol conc., 0.0532 mol/liter.

lecular weight of the polymer and other species (i) is neglected. The total molar concentration of reactive polymer may then be written as

$$\sum_n c(P_n) = \frac{M_{\mathrm{PhOH}}}{\overline{M}_n} \cdot (c_{\mathrm{PhOH},0} - c_{\mathrm{PhOH}}) - \sum_i \frac{1}{\nu_i} \cdot \frac{M_i}{\overline{M}_n} \cdot c_i, \quad (3)$$

where $\overline{M}_n$, the number average molecular weight, is defined as

$$\overline{M}_n = (M_{\mathrm{PhOH}} + M_{\mathrm{Gly}}) \cdot \frac{\sum_n n \cdot c(P_n)}{\sum_n c(P_n)}. \quad (4)$$

In Eq. (4) it is stated that the polymer consti-

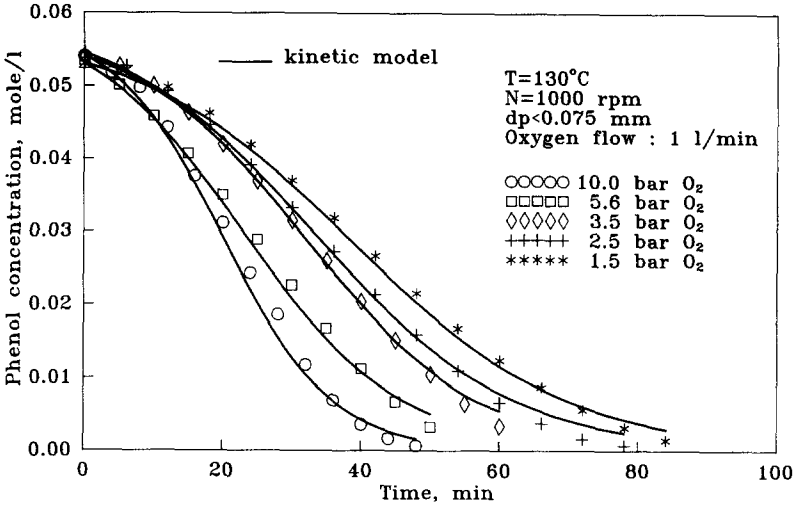

FIG. 5. Residual phenol concentration as a function of time at different oxygen partial pressures and T = 130°C. Cat. conc., 5 g/liter. Initial phenol conc., 0.0532 mol/liter.

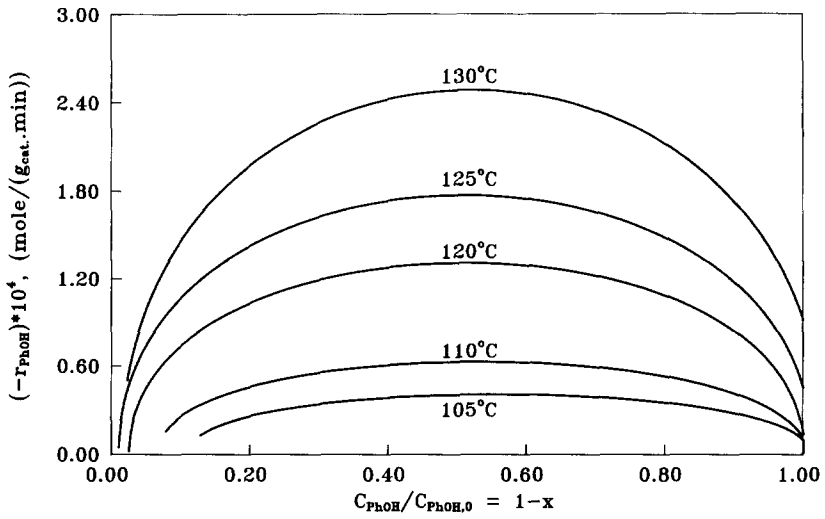

FIG. 6. Phenol oxidation rate vs dimensionless concentration at different temperatures.

tutes an equal number of phenol and glyoxale molecules.

The rate expression may now be obtained by use of Eqs. (1) and (3), namely,

$$-r_{PhOH} = k^* \cdot c_{PhOH} \cdot \left[1 + \frac{k \cdot M_{PhOH}}{k^* \cdot \overline{M}_n} \cdot c_{PhOH,0} - \frac{k}{k^*} \cdot \sum_i \frac{1}{\nu_i} \cdot \frac{M_i}{\overline{M}_n} \cdot c_i - \frac{k \cdot M_{PhOH}}{k^* \cdot \overline{M}_n} \cdot c_{PhOH} \right], \quad (5)$$

where the rate constant k^* is a product of k' and $f(p(O_2))$. Equation (5) may be further reduced to the form

$$-r_{PhOH} = k^* \cdot c_{PhOH} \cdot \left(c_0 - \frac{k \cdot M_{PhOH}}{k^* \cdot \overline{M}_n} \cdot c_{PhOH} \right), \quad (6)$$

where the dimensionless empirical constant c_0 is defined as

$$c_0 = 1 + \frac{k \cdot M_{PhOH}}{k^* \cdot \overline{M}_n} \cdot c_{PhOH,0} - \frac{k}{k^*} \cdot \sum_i \frac{1}{\nu_i} \cdot \frac{M_i}{\overline{M}_n} \cdot c_i. \quad (7)$$

If one assumes that c_0 and $\overline{M}_n$ are not dependent on the phenol conversion, Eq. (6) on appropriate integration yields

$$\ln \frac{c_{PhOH,0} \cdot \left(c_0 - \frac{k \cdot M_{PhOH}}{k^* \cdot \overline{M}_n} \cdot c_{PhOH} \right)}{c_{PhOH} \cdot \left(c_0 - \frac{k \cdot M_{PhOH}}{k^* \cdot \overline{M}_n} \cdot c_{PhOH,0} \right)} = k^* \cdot c_0 \cdot c_{cat.} \cdot t. \quad (8)$$

Statistical analysis of the experimental data by a nonlinear regression method alludes that the ratio $(k \cdot M_{PhOH}/k^* \cdot \overline{M}_n)$ is more or less constant and its value is close to one. It was also found out that a value of the constant (c_0) is slightly greater than $c_{PhOH,0}$ (approximately 10%). However, for the sake of simplicity the ratio was fixed at a value of 1.0; consequently, Eq. (8) further reduces to

$$\ln \frac{c_{PhOH,0} \cdot (c_0 - c_{PhOH})}{c_{PhOH} \cdot (c_0 - c_{PhOH,0})} = k^* \cdot c_0 \cdot c_{cat.} \cdot t, \quad (9)$$

which is, in fact, the integrated rate expression for an elementary autocatalytic reaction. Thus, as discussed in the previous section, the autocatalytic behavior of the reaction system may be ascribed to a homo-

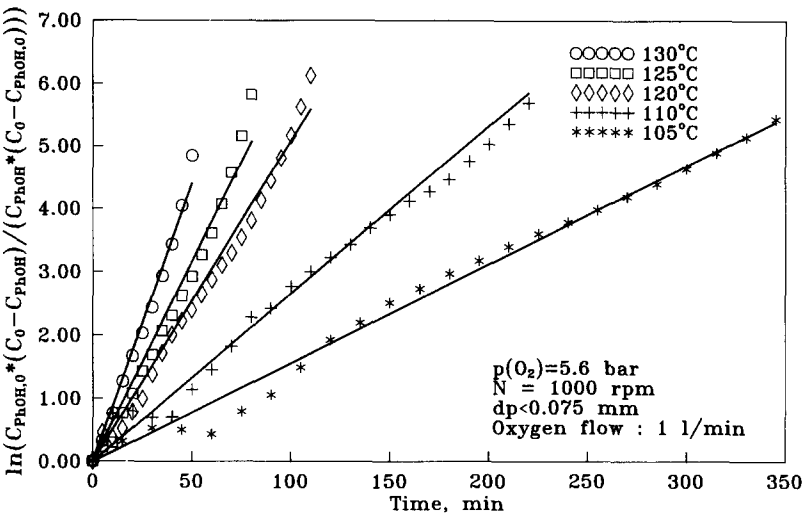

FIG. 7. Test of assumed kinetic model for an autocatalytic reaction.

geneous reaction between residual phenol (PhOH) and a polymer (P_n).

To test for the proposed kinetic model the experimental results from Fig. 4 must be plotted according to Eq. (9) to see whether a straight line passing through zero can be obtained. This is illustrated in Fig. 7 where the above condition is obviously fulfilled. Slight deviations of the experimental points, from the lines obtained by a regression method, are attributed to temperature oscillation in the reactor. Assuming c_0 and $\overline{M}_n$ to be constant seems to be responsible for more pronounced deviations at higher temperatures and high phenol conversions. From the slopes of straight lines a temperature dependence of k^* was determined with a plot of $\ln(k^*)$ vs $(1/T)$ shown in Fig. 8 (Curve 1). The apparent activation energy of 84 kJ/mol is calculated for the phenol oxidation over $CuO \cdot ZnO \cdot Al_2O_3$ catalyst. The value is much lower than 176 kJ/mol, which was found for the same reaction catalyzed by CuO on γ-Al_2O_3 (*8*). On the other hand, it is in good agreement with the activation energies found for the liquid-phase catalytic oxidation of pure hydrocarbons (*3*), and the result of Ohta *et al.* (85.3 kJ/mol) (*10*).

The effect of oxygen partial pressure on k^*, i.e., on the oxidation rate, is illustrated in Fig. 9. Values of k^* at different oxygen partial pressures were calculated from the data presented in Fig. 5. As can be seen a power of 0.25 on the oxygen partial pressure fits the experimental data quite well. The experimental data point near the diagram origin (Fig. 9) was obtained with pure nitrogen flowing through the reactor. This point can be considered as a test of the experimental consistencies. Evaporation of the aqueous solution, and consequently possible change of the phenol concentration, has not contributed significantly to an experimental error. Furthermore, the data point also suggests that the catalyst lattice oxygen does not contribute to the phenol oxidation, indicating that a redox reaction mechanism can be excluded. However, orders of 0.5 and 1.0 with respect to oxygen partial pressure were found in acetic and formic acid oxidation, respectively. In liquid-phase phenol oxidation over CuO on γ-Al_2O_3 the order was determined to be nearly 0.5 (*8, 10*). In the oxidation of pure organic substances there is considerable information (*3*) indicating that the oxygen partial pressure does not affect the rate as long as this pressure is greater

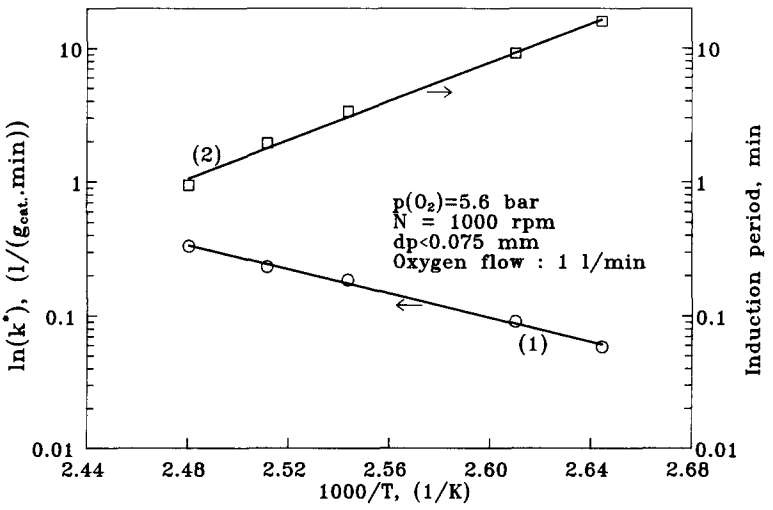

FIG. 8. Temperature dependence of rate constant k^* and induction period for phenol oxidation. Cat. conc., 5 g/liter.

than about 100 mm Hg. An order of 0.25 found here, which is rare, probably results from the fact that phenol disappears by homogeneous and heterogeneous reactions, while oxygen only by the latter.

In Fig. 10 k^* is plotted against the catalyst concentration. It is seen that $k^* \cdot c_{cat.}$ (Curve 2) increases linearly with the catalyst concentration. At higher catalyst loadings the rate would probably decrease (*3, 9, 10*). It is also evident that the extrapolation of Curve 2 to zero catalyst concentration does not yield a value of $k^* \cdot c_{cat.}$ equals zero. This may be attributed to a possible homogeneous initiation of radicals, promoted by cupric ions in the solution, leached from the

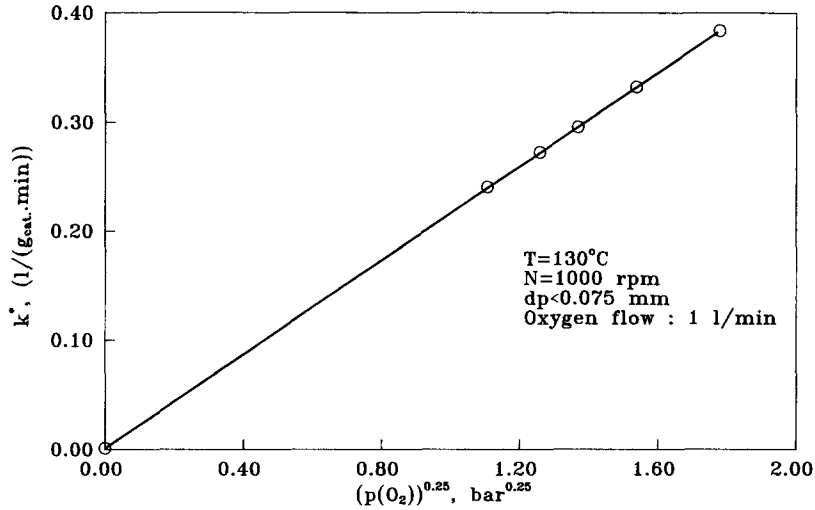

FIG. 9. Rate constant k^* as a function of oxygen partial pressure. T = 130°C. Cat. conc., 5 g/liter. Initial phenol conc., 0.0532 mol/liter.

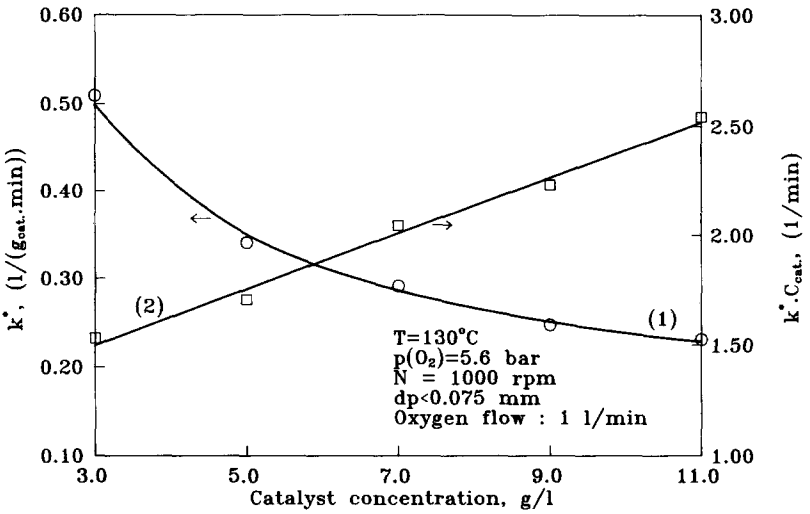

FIG. 10. Rate constant k^* as a function of catalyst concentration. Initial phenol conc., 0.0532 mol/liter.

catalyst (75 mg/liter in this work) (*15*). The impact of initial phenol concentration on the oxidation rate (k^*) is illustrated in Fig. 11. An obvious inhibition effect of the initial phenol concentration is demonstrated. A positive dependence of the reaction rate on catalyst concentration and inhibition effect of the initial phenol concentration suggests that termination steps occur on the catalyst surface and in the liquid phase probably by self-inhibition.

Equation (9) can be used to predict the concentration of phenol as a function of time. Such predictions are shown in Figs. 4 and 5 by solid curves. Disagreement between the experimental data and predictions increases as temperature decreases (Fig. 4). Since the catalytic oxidation of phenol undergoes a free radical mechanism, the disagreement can be attributed to an induction period which is not accounted for in Eq. (1). At high temperatures the rate of radical (and thus also glyoxale as an initiator) formation is high enough that reaction proceeds immediately. It should be recalled that a constant concentration of radicals was assumed in developing Eq. (9), but that it is undoubtedly dependent on temperature. Consequently, a poor agreement can be expected at lower temperatures. However, it is obvious that the experimental data points can be well fitted if the predicted curves are shifted to the right for a time increment corresponding to the induction period. Adjusting the loci of curves to the experimental data yields the values of induction period as a function of temperature. This dependence is illustrated in Fig. 8 (Curve 2).

CONCLUSIONS

The catalytic phenol oxidation in aqueous solution involves a heterogeneous–homogeneous free radical mechanism. Radicals are probably initiated on the catalyst surface and play a role in the oxidation route toward glyoxale formation.

The rate of phenol disappearance can be well described by a rate equation which corresponds to an autocatalytic reaction. The rate in a slurry system is proportional to the oxygen partial pressure with a power of 0.25 and linear proportional to the catalyst concentration. The rate also depends on the initial phenol concentration.

It is assumed that ring opening, and consequently the glyoxale formation, is the rate-controlling step in the catalytic phenol oxidation. A polymeric product, which de-

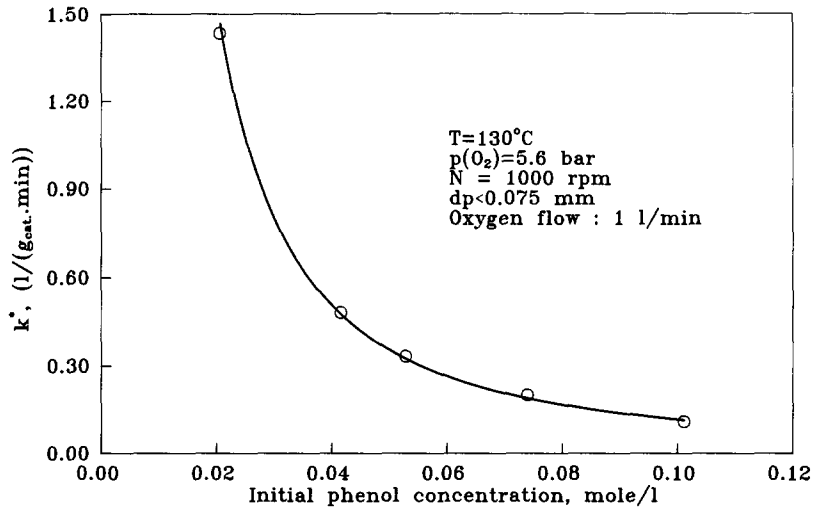

FIG. 11. Rate constant k^* as a function of initial phenol concentration. Cat. conc., 5 g/liter.

activates the catalyst, mainly arises from the stepwise addition of phenol to a polymer initially formed by the reaction between glyoxale and phenol. Glyoxale can be considered as an initiator in the polymerization reaction. Slightly more than one-third of the initial phenol amount is oxidized to carbon dioxide, and the rest forms a nontoxic polymeric product.

APPENDIX: NOTATION

$c_{cat.}$	catalyst concentration (g/liter)
c_i	concentration of intermediate and product species i (mol/liter)
c_{PhOH}	phenol concentration (mol/liter)
$c_{PhOH,0}$	initial phenol concentration (mol/liter)
c_0	empirical constant
$\Sigma_n\, c(P_n)$	total concentration of all polymers of all possible chain lengths (mol/liter)
$\Sigma_n\, n \cdot c(P_n)$	first moment of the $c(P_n)$ (mol/liter)
E_a	apparent activation energy (kJ/mol)
k	lump polymerization rate constant (liter^2/(mol $\cdot$ $g_{cat.}$ $\cdot$ min))
k'	heterogeneous rate constant (liter/($g_{cat.}$ $\cdot$ min $\cdot$ bar^m))
k^*	apparent heterogeneous rate constant (liter/($g_{cat.}$ $\cdot$ min))
M_{Gly}	molecular weight of glyoxale (g/mol)
M_i	molecular weight of intermediate and product species i (g/mol)
M_n	molecular weight of a polymer composed of n monomer molecules (g/mol)
$\overline{M}_n$	number average molecular weight (g/mol)
M_{PhOH}	molecular weight of phenol (g/mol)
$p(O_2)$	oxygen partial pressure (bar)
R	gas constant (J $\cdot$ mol^{-1} $\cdot$ K^{-1})
$(-r_{PhOH})$	phenol oxidation rate (mol $\cdot$ $g_{cat.}^{-1}$ $\cdot$ min^{-1})
T	temperature (K)
t	time (min)
x	phenol conversion
ν_i	general stoichiometric coefficient

ACKNOWLEDGMENT

The authors acknowledge support from the EC under Grant CI1*-CT90-0623 and the Research Council of Slovenia under Grant C2-2541-104. The authors also thank Dr. J. Kobe for helpful discussions, Dr. A. Sebe-

nik for taking the NMR spectra, and Süd-Chemie AG, Munich, for supplying the catalyst samples.

REFERENCES

1. Ollis, D. F., Pelizzetti, E., and Serpone, N., *in* "Photocatalysis: Fundamentals and Applications" (N. Serpone and E. Pelizzetti, Eds.), p. 603. Wiley, New York, 1989.
2. Farha, E. F., Box, E. O., Jr., Dunn, R. O., and Kuerston, R. D., *Prepr. Div. Pet. Chem. Am. Chem. Soc.* **23**(1), 93 (1978).
3. Goto, S., Levec, J., and Smith, J. M., *Catal. Rev. Sci. Eng.* **15,** 187 (1977).
4. Katzer, J. R., Ficke, H. H., and Sadana, A., *J. Water Pollut. Control Fed.* **48,** (5), 920 (1976).
5. Baldi, G., Goto, S., Chow, C. K., and Smith, J. M., *Ind. Eng. Chem. Process Des. Dev.* **13** (4), 447 (1974).
6. Levec, J., and Smith, J. M., *AIChE J.* **22**(1), 159 (1976).
7. Levec, J., Herskowitz, M., and Smith, J. M., *AIChE J.* **22**(5), 919 (1976).
8. Sadana, A., and Katzer, J. R., *Ind. Eng. Chem. Fundam.* **13**(2), 127 (1974).
9. Sadana, A., and Katzer, J. R., *J. Catal.* **35,** 140 (1974).
10. Ohta, H., Goto, S., and Teshima, H., *Ind. Eng. Chem. Fundam.* **19**(2), 180 (1980).
11. Levec, J., German Patent Application P 39 38 835.2 (1989).
12. Levec, J., *Appl. Catal.* **63**(1), L1 (1990).
13. Golodec, G. I., "Geterogenno-kataliticeskoe okislenie organiceskih vesestv," p. 295. Naukova Dumka, Kiev, 1978.
14. Shibaeva, L. V., Metelitsa, D. I., and Denisov, E. T., *Kinet. Katal.* **10**(5), 1020 (1969).
15. Njiribeako, A. J., Hudgins, R. R., and Silveston, P. L., *Ind. Eng. Chem. Fundam.* **17**(3), 234 (1978).